Human Thymidylate Synthase Is in the Closed Conformation When Complexed with dUMP and Raltitrexed, an Antifolate Drug[†,‡]

Jason Phan,[§] Sangita Koli,[§,||] Wladek Minor,[⊥] R. Bruce Dunlap,[§] Sondra H. Berger,[||] and Lukasz Lebioda*[,§]

Departments of Chemistry and Biochemistry, Biological Sciences,and Basic Pharmaceutical Sciences, University of South Carolina, Columbia, South Carolina 92908, and Department of Molecular Physiology and Biological Physics, University of Virginia, Charlottesville, Virginia 22901

Received October 17, 2000; Revised Manuscript Received December 11, 2000

ABSTRACT: Thymidylate synthase (TS) is a major target in the chemotherapy of colorectal cancer and some other neoplasms while raltitrexed (Tomudex, ZD1694) is an antifolate inhibitor of TS approved for clinical use in several European countries. The crystal structure of the complex between recombinant human TS, dUMP, and raltitrexed has been determined at 1.9 Å resolution. In contrast to the situation observed in the analogous complex of the rat TS, the enzyme is in the closed conformation and a covalent bond between the catalytic Cys 195 and dUMP is present in both subunits. This mode of ligand binding is similar to that of the analogous complex of the *Escherichia coli* enzyme. The only major differences observed are a direct hydrogen bond between His 196 and the O4 atom of dUMP and repositioning of the side chain of Tyr 94 by about 2 Å. The thiophene ring of the drug is disordered between two parallel positions.

Thymidylate synthase (TS)[1] catalyzes the reductive methylation of 2′-deoxyuridine 5′-monophosphate (dUMP) to thymidine 5′-monophosphate (dTMP), using the cosubstrate 5,10-methylenetetrahydrofolate (CH_2H_4folate) as a one-carbon donor and reductant. This reaction is the only de novo source of thymidylate (*1*). The inhibition of TS in rapidly dividing cells leads to pronounced changes in cellular protein and RNA, cessation of DNA replication, and eventually cell death, a phenomenon termed thymineless death (*2*). This makes TS uniquely suited as a target for cancer chemotherapy and protocols utilizing TS inhibitors have been used in the clinic for over 30 years. A commonly prescribed chemotherapeutic drug is 5-fluorouracil, which is a potent inhibitor of TS after metabolism to 5-fluoro-dUMP (FdUMP) (*3*). In recent years, analogues of the other substrate, collectively termed antifolates, emerged as a new class of TS-targeted agents (*4*). Many of them are in different stages of clinical trials, with raltitrexed (Tomudex, ZD1694) already approved for the therapy of advanced colorectal cancer in several European countries (*5*). In cells, raltitrexed undergoes enzymatic polyglutamylation to tri- and pentaglutamates in a reaction catalyzed by folylpolyglutamate synthetase (FPGS). Polyglutamylation is an important determinant of the cytotoxicity of raltitrexed since it decreases the binding constant of hTS and increases cellular retention; about 80% of intracellular drug is in the polyglutamylated form (*6*). In some clinical studies, raltitrexed efficacy was similar to that of fluorouracil/leucovorin protocols and produced lesser toxicity (*5*). This appears to be especially true if patients with low levels of FPGS and/or high levels of γ-glutamyl hydrolase (GGH), an enzyme that removes glutamyl residues, are eliminated from trials.

Crystallographic studies of TS complexes with raltitrexed have been carried out with *Escherichia coli* TS (ecTS) at 2.2 Å resolution (*7*) and with rat TS (rTS) at 2.6 Å resolution (*8*). While the ecTS/dUMP/raltitrexed complex crystallized in the closed conformation, with a covalent bond between the catalytic cysteine and C(6)-atom of dUMP, the TS conformation in the rTS/dUMP/raltitrexed complex was not closed and the covalent bond was not present. Crystal structures of complexes of human thymidylate synthase (hTS) have not been reported due to problems in obtaining suitable crystals. However, the structure of unliganded hTS has been determined (*9*, *10*) and an unusual conformation was observed. The active-site loop, residues 181−197, is rotated approximately 180° with respect to its orientation in bacterial TSs. The sulfhydryl group of the catalytic nucleophile, Cys 195, is not located in the active site, but more than 10 Å

[†] This work was supported by NIH Grant CA 76560 and the South Carolina Cancer Center. Some instrumentation used in this research was purchased with NSF Grant BIR 9419866 and DOE Grant DE-FG-95TE00058.

[‡] The PDB file with atomic coordinates of recombinant hTS complexed with dUMP and raltitrexed (Tomudex or ZD1694) has been deposited in the Protein Data Bank as entry 1HVY.

* To whom correspondence should be addressed. Phone (803) 777-2140. Fax: (803) 777-9521. E-mail: lebioda@mail.chem.sc.edu.

[§] Departments of Chemistry and Biochemistry and Biological Sciences.

[||] Department of Basic Pharmaceutical Sciences.

[⊥] Department of Molecular Physiology and Biological Physics.

[1] Abbreviations: TS, thymidylate synthase; hTS, human thymidylate synthase; ecTS, *Escherichia coli* thymidylate synthase; dUMP, 2′-deoxyuridine 5′-monophosphate; dTMP, 2′-deoxythymidine 5′ monophosphate; CH_2H_4folate, 5,10-methylenetetrahydrofolate; raltitrexed, Tomudex or ZD1694, *N*-(5-[*N*-(3,4-dihydro-2-methyl-4-oxoquinazolin-6-ylmethyl)-*N*-methylamino]-2-thenoyl)-L-glutamic acid; FdUMP, 5-fluoro-2′-deoxyuridine 5′-monophosphate; EDTA, ethylenediaminetetraacetic acid; 2-ME, 2-mercaptoethanol; PMSF, phenylmethanesulfonyl fluoride; DTT, dithiothreitol; Tris, tris(hydroxymethyl)aminomethane; H_4folate, (+)-tetrahydrofolate; PEG, poly(ethylene glycol); PDB, Protein Data Bank.

10.1021/bi002413i CCC: $20.00
Published on Web 01/23/2001

from the corresponding position in bacterial enzymes; thus, in this conformation, the enzyme must be inactive. This inactive conformer has not been observed in any other TS, and conversely, the structures of hTS previously reported have not been in either an active conformation or a liganded form. Recently, we were able to obtain suitable crystals that allowed us to elucidate the structure of the hTS/dUMP/raltitrexed complex at 1.9 Å resolution. While many inhibitory complexes of TS have been studied by crystallography, this is the first report of a complex of the human enzyme. It shows that for enzymes, even as conserved as TS, differences between proteins from different species may have significant impact on the efficacy of drug design.

EXPERIMENTAL PROCEDURES

Materials. Raltitrexed was obtained from AstraZeneca. Nucleotides, salts, 2-mercaptoethanol (2-ME), phenylmethanesufonyl fluoride (PMSF), ethylene glycol, poly(ethylene glycol)s (PEGs), folic acid, and tris(hydroxymethyl)aminomethane (Tris) were obtained from Sigma (St. Louis, MO). Formaldehyde was purchased from Fisher (Pittsburgh, PA). Culture plate used in crystallization was from Corning Inc. (Corning, NY). Ultrapure ammonium sulfate was from ICN Biomedicals, Inc. (Aurora, OH). Centriprep-30 concentrators were purchased from Amicon (Beverly, MA). Restriction enzymes and T4 DNA ligase were from New England Biolabs (Beverly, MA). (6*S*)-5,6,7,8-tetrahydrofolic acid (H_4folate) was prepared from folic acid and converted to (6R)-CH_2H_4folate as described previously (*11*).

Expression and Purification of Human Thymidylate Synthase. Recombinant hTS was expressed as described previously (*12*). Transformed bacteria cells were grown in Luria Bertani broth and used to inoculate 1 L cultures containing 100 μg/mL ampicillin. The cultures were incubated for 12−16 h; cells were harvested by centrifugation at 1000*g* at 4 °C and frozen at −70 °C. Cell pellets (2−3 g) were thawed on ice and suspended in buffer A (50 mM Tris-base, 1 mM EDTA, and 14 mM 2-ME at pH 7.4 and 4 °C) containing 0.1 mM PMSF. Cells were lysed at 4 °C by sonication using a Branson Sonifier 450 (Branson Ultrasonics, Danbury, CT). Cell debris was removed by centrifugation at 18000*g* at 4 °C for 30 min. The cell extract was loaded onto a Blue Sepharose CL-6B column (Pharmacia) and washed with buffer A. The fractions containing the enzyme were eluted from the column using buffer B (buffer A with 100 mM KCl), pooled and dialyzed overnight against buffer A (*12*). Purified hTS was analyzed by 12% SDS−PAGE for purity and stored in buffer A containing 15% glycerol at −20 °C.

Protein Determination and Catalytic Assay. Enzyme activity was measured spectrophotometrically by monitoring the absorbance change accompanying the conversion of CH_2H_4folate to H_2folate (*13*) using either a Shimadzu UV 1601 spectrophotometer equipped with a TCC 240A temperature-controlled cell holder or a Shimadzu UV 2101 PC spectrophotometer (Shimadzu Corporation, Columbia, MD). Measurements were carried out at 25 °C and pH 7.4 in Morrison buffer (*14*). One unit of enzyme activity is defined as the amount of enzyme required to synthesize 1 μmol of dTMP/min. Enzyme concentration was determined by measurement of absorbance at 280 nm, as described previously (*15*).

Crystallization of the Ternary Inhibitory Complex of Human Thymidylate Synthase. Crystals of recombinant hTS complexed with dUMP and raltitrexed were grown by the vapor diffusion method in the hanging drop setup in tissue culture plates. In the drop, 5 μL of ternary complex solution (5.3 mg/mL) containing 1 mM EDTA, 10 mM 2-ME, and 200 mM Tris-base (pH 8.8) was mixed with an equal volume of precipitant solution containing 40% PEG 4K, 2% saturated ammonium sulfate, 20 mM 2-ME, and 100 mM Tris-HCl (pH 7.6) and allowed to equilibrate with 0.6 mL of precipitant solution in the well. The culture plates were stored undisturbed in the dark at room temperature, and thin plate-shaped crystals of dimensions 0.06 × 0.15 × 0.50 mm were observed after 3−4 weeks.

Diffraction Data Measurement, Processing, and Structure Determination. A complete set of oscillation data were measured on a single crystal of hTS/dUMP/raltitrexed. The crystal was mounted directly from the cryogenic mother liquor and flash-cooled in N_2 vapors at −178 °C. The crystallographic diffraction experiment was carried out using CuKα radiation of 1.5418 Å in wavelength generated by a rotating anode. Reflection data were collected with the Raxis IV area detector at a crystal to detector distance of 120 mm and processed with Denzo/Scalepack software (*16*). The atomic coordinates of the structure of native hTS (to be published) were used as the search model in molecular replacement by aMoRe (*17*) in the CCP4 suite of programs (*18*). The rotation function applied to the hTS/dUMP/raltitrexed data utilizing phasing solutions from the unliganded hTS model showed four 2-fold related peaks, corresponding to four monomers. Thus, the internal 2-fold axis was used to generate a dimer from the initial monomeric model. The highest cross-rotational peak was oriented to one dimer followed by a translational search in the absence of the second dimer. Rigid body refinement of the solutions resulted from the translational search yielded an R_{crys} of 0.48. The fitted tetramer was subject to simulated annealing using torsional angle dynamics, positional and individual temperature factor refinements using the CNS software (*19*). Electron density maps calculated with $2F_o - F_c$ and $F_o - F_c$ coefficients were utilized to introduce manual corrections to the model with the interactive graphics program CHAIN (*20*). Least-squares superpositions of structures were based on positions of C_α of subunit A and carried out in an iterative manner to include only those equivalencies for which distances were less than 2.0 Å. Calculations were carried out using the LSQKAB software (*21*) from the CCP4 suite of programs (*18*). Ribbon diagrams and wire-and-basket models were prepared with the programs MOLSCRIPT (*22*) and CHAIN (*20*), respectively.

RESULTS

Crystallization. Crystals of the ternary complex of the enzyme did not grow in the typical high-salt conditions favored by native hTS and bacterial TSs. However, with moderate pH change and low ionic strength, these crystals were successfully grown to suitable sizes in poly(ethylene glycol) 4000. They are plate-shaped and stacked end-on into a long multiple crystal. The single-crystal belongs to the space group *P*1 with two dimers in the asymmetric part of the unit cell. The crystal parameters and statistics of crystallographic refinements are summarized in Table 1.

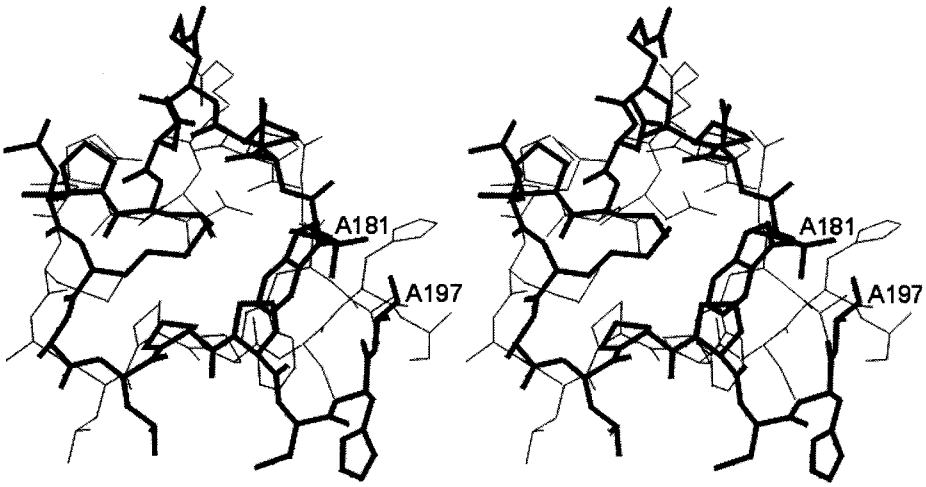

FIGURE 1: Stereoview of a least-squares superposition of loop 181−197 in the active conformation (in heavy lines) and in the inactive conformation.

Table 1: Crystal Parameters and Refinement Statistics

space group	*P*1
a (Å)	68.85
b (Å)	70.50
c (Å)	74.53
α (deg)	70.23
β (deg)	83.30
γ (deg)	73.28
mosaicity (deg)	0.59
resolution (Å)	1.9
reflections, measured	229 821
reflections, independent	94 011
completeness (%)	93.8
R_{sym}[a]	0.072
R_{crys}[c]/R_{free}	0.20/0.24
average *B* (Wilson plot)	10.5
most favored *φ*/*ψ* (%)	87.4
rmsd, bond lengths (Å)	0.006
rmsd, bond angles (deg)	1.3
rmsd, in Cα[d]	0.16
no. solvent molecules	601
no. ligand ions/molecules	12

[a] $R_{sym} = (\sum_h|I_h - \langle I\rangle|)/(\sum_h I_h)$. [c] $R_{crys} = (\sum_h|F_{obs} - F_{cal}|)/(\sum_h F_{obs})$. R_{free} = crystallographic *R*-factor for test set as implemented in CNS_1.0 (*19*). [d] Root-mean-square deviation.

Overall Structure. The data, having a mosaicity of 0.59 and an overall R_{merge} of 0.072, yielded excellent electron density maps; there is continuous density from Pro 26 to Ala 312 in all four subunits. The structure of hTS/dUMP/raltitrexed complex is similar to those of rat and *E. coli* TS complexes as is expected from the highly conserved primary structures. As reported for the rTS complex (*8*), the inserts specific for mammalian TSs are in a well-defined conformation. The N-terminal extension is largely disordered; good density starts at Pro 26, as was observed in native hTS and in the inhibitory ternary complex of rTS (PDB entry 2tsr, ref *8*). The active site loop is in the active conformation as was also found in the rTS/dUMP/raltitrexed complex (*8*). Its superposition on the loop in the inactive conformation of the native hTS yielded a root-mean-square (rms) deviation between C_α of 2.4 Å (for residues 182−197). The superposition, shown in Figure 1, indicates that the major conformational differences are essentially limited to the hinge regions. Unlike in the rTS complex, in the hTS complex, the C-terminus is ordered and its structure resembles closely those observed in bacterial TS inhibitory ternary complexes. The exception to this is the last residue, Val 313. In the ecTS complex the terminal carboxylate forms an ion pair with an arginine (ecTS Arg 21), which corresponds to Arg 50 in hTS. In the hTS complex, Val 313 shows poor density and the dominant form has the carboxylate away from the guanidinium moiety of Arg 50.

Superpositions of Structures. There are two dimers per asymmetric part of the unit cell; the subunits of the first molecule are denoted A and B while C and D form the other molecule. Subunits B, C, and D were superimposed on subunit A and yielded rms deviations between the C_α positions of 0.29, 0.27, and 0.29 Å. A least-squares superposition of the unliganded hTS, based on residues 27−49, 54−102, 132−182, and 196−310 yielded an rms distance between C_α positions of 0.64 Å. A superposition of the complex rTS/dUMP/raltitrexed (PDB entry 2tsr, ref *8*) subunits C and D, which had better density than A and B (*8*) to residues 27−303 of the hTS complex, subunit A, yielded rms distances between C_α positions of 0.61 and 0.50 Å, respectively. Two bacterial complexes, each with two subunits per asymmetric cell, also were compared to the hTS/dUMP/raltitrexed complex: the ecTS/FdUMP/CH_2H_4folate complex (PDB entry 1tls, ref *23*) and the ecTS/dUMP/raltitrexed complex (PDB entry 2kce, ref *7*). The equivalencies used for them were hTS 30−110, 129−142, and 157−310; they yielded very similar rms distances between C_α, all in a range 0.73−0.75 Å.

Ligand Binding. There is excellent density for the dUMP and raltitrexed molecules in all four subunits (Figure 2) and the temperature factors are very similar to those of the neighboring protein atom, indicating full occupancy of the binding sites. An exception to this is the glutamate tail of raltitrexed, which appears to be disordered between two quite well-defined positions.

There is continuous density between C6 of dUMP and S_γ of Cys 195 indicating covalent bonding, and the distances are consistent with such assessment. The position of the dUMP molecule is very similar to the positions of nucleotide ligands present in the ecTS/dUMP/raltitrexed and ecTS/FdUMP/CH_2H_4folate complexes. In contrast, the position of dUMP in rTS/dUMP/raltitrexed is shifted 0.4−0.7 Å away from the catalytic cysteine, which is consistent with the interpretation (*8*) that the complex is noncovalent. The sole

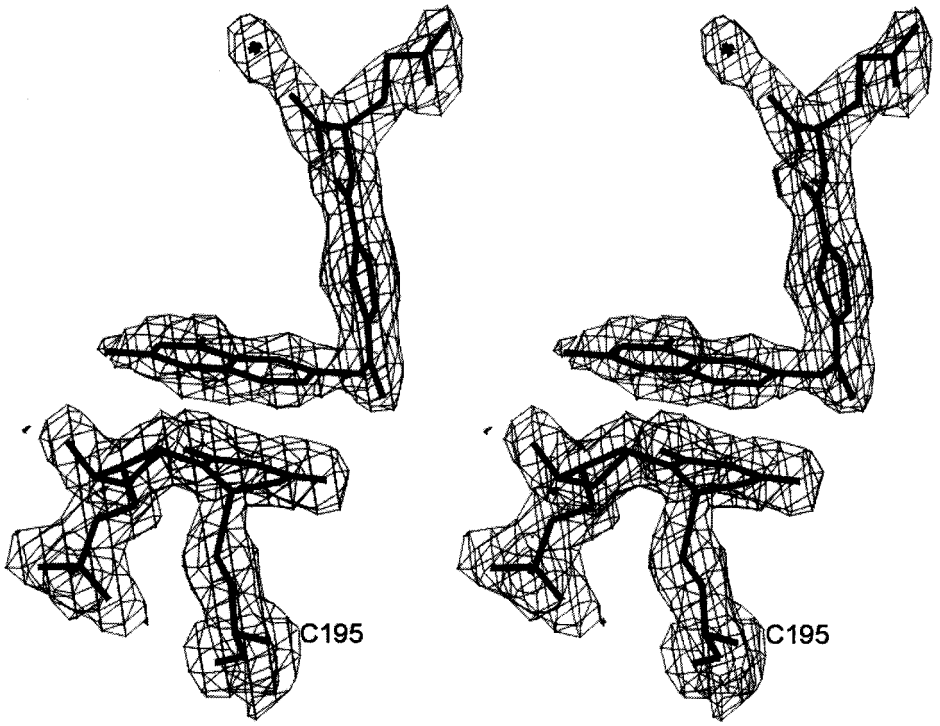

FIGURE 2: Stereoview of electron density contoured at 1.0σ for the catalytic cysteine, Cys 195, and the ligands: dUMP in the middle and raltitrexed, on the top. The glutamate tail appears to be disordered between two positions.

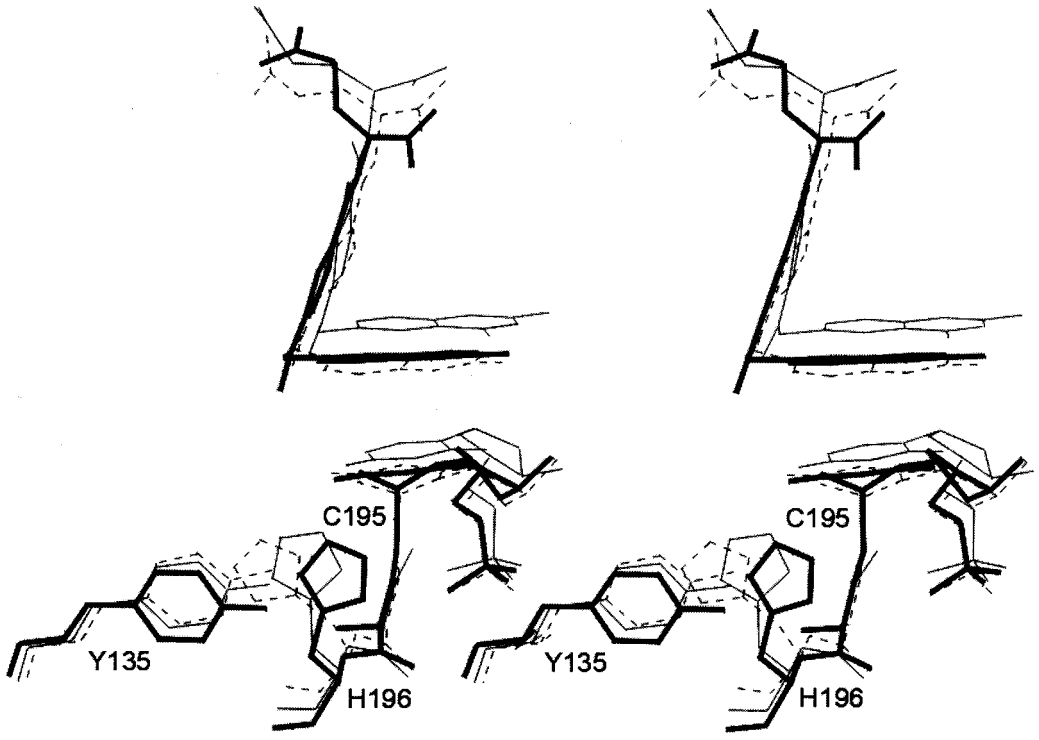

FIGURE 3: Stereoview of a superposition of the structures of TS complexes with dUMP and raltitrexed. In heavy line is the hTS complex, in single line rTS, and in dash line ecTS. The superposition is entirely based on the positions of C_α; see text for the equivalencies. The fit between ecTS and hTS is superb and the major structural differences are significant. The differences between rTS and hTS are entirely consistent with the presence of covalent bond in the hTS complex and its absence in the rTS complex.

major difference at the nucleotide-binding site between the bacterial and mammalian complexes is the position of His 196. In complexes of mammalian species, there is a direct interaction between the His 196 imidazole and the O4 atom of the nucleotide. In contrast, in the complexes of ecTS the interaction is not direct but mediated through a conserved water molecule, also coordinated to Glu 87 (ecTS Glu 58). This water molecule is also present in the mammalian TS complexes but it does not form a hydrogen bond with the side chain of His 196. This is due to a difference in the main-chain conformation, which results in repositioning of the His 196 imidazole and formation of a direct hydrogen bond between $N^{\epsilon 2}$ and O4. The environment of $N^{\delta 1}$ is nonpolar and it is unlikely that this atom is protonated. The different

position of His 196 is correlated with the position of the side chain of Tyr 135. In ecTS complexes the equivalent Tyr 94 is stacked against the imidazole and its phenolic oxygen is an acceptor of a hydrogen bond from the backbone N-atom of catalytic Cys 146. In mammalian enzymes, the position of O^{η} is 1.9 Å away and it accepts a H-bond from the N-atom of His 196. The other significant difference between ecTS and hTS is a hydrophobic interaction between the side chain of Met 313 and the 2-desamino-2methyl quinazoline moiety. In the ecTS complex, the residue equivalent to Met 313, Val 261, is not in contact with the bound raltitrexed molecule while in the hTS complex the $S_{\delta}-N1$ distance is 3.0 Å. It is likely that this interaction, which perhaps involves charge transfer between a lone electron pair of S_{δ} and the quinazoline aromatic system, is responsible for the tighter binding of raltitrexed by the human enzyme than by ecTS (*7*).

The open versus closed conformations of rTS/dUMP/raltitrexed and hTS/dUMP/raltitrexed complexes led to significant differences in the position of the nucleotide in the active site. Differences between the positions of the raltitrexed ligand are even larger, 0.5−1.0 Å, as the position of the 2-desamino-2methyl quinazoline ring system is shifted and tilted away from the pyrimidine ring (Figure 3). Difference electron density maps (not shown) revealed the presence of positive peaks at C16 of the thiophene ring in all subunits. It is an indication of disorder of the thiophene ring between two positions flipped by 180°, with the heavier sulfur atom generating the extra density.

Can a more tightly binding ligand be designed based on the structure of the complex? One area that appears to be worth testing is the replacement of the N−H moiety of the glutamate with a CH_2 moiety. The peptide imino group does not have an acceptor for its hydrogen bond function (Figure 4) and its transfer form water to hydrophobic environment must be energetically unfavorable. The other possibilities are at C8 atom, which does not form contacts, and obviously at CP1, where a propargyl substituent was successfully used in CB3717.

DISCUSSION

Although there are important differences between the structures of the rat rTS/dUMP/raltitrexed and the corresponding complex of the human enzyme, there are many features that are common. Their presence in both complexes and actually in five different crystal environments (three rat dimers and two human dimers) essentially allows one to eliminate the "crystal field effect" from considerations. Protein molecules are typically slightly distorted at contacts with other molecules forming a crystal. However, when structures in multiple crystal forms, or several crystalografically independent subunits are available, contacts are different and distortions are also different. Thus when multiple observations are made, it is higly likely that the common structural features reflect the situation in solution. This is especially important for analyses of the ordered versus disordered fragments of the molecule since crystal contacts may stabilize ordered forms and significantly shift conformational equilibria. The primary structure of hTS differs from that of ecTS in three regions: the N-terminus of hTS is extended by 29 residues and two insertions of 12 and 8

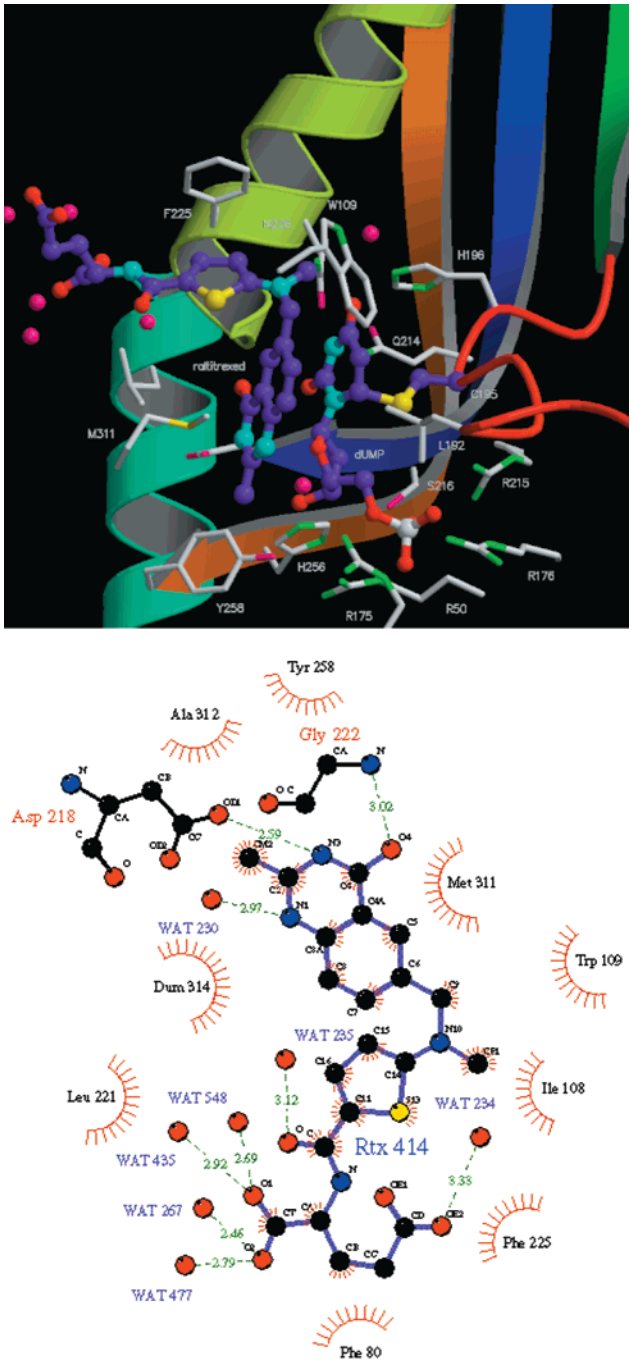

FIGURE 4: (Top) Environment of raltitrexed drawn with the program MOLSCRIPT (*25*). The ligands, raltitrexed and dUMP, are in purple; side chains are in silver, while the main chain representation reflects its secondary structure. (Bottom) Schematic diagram of the ligand environment as displayed by the program LIGPLOT (*26*). The bonds of raltitrexed (Rtx) are displayed in purple and those of the protein in black. Hydrogen bonds are green dashes with the bond length noted. Protein residues and ligand atoms involved in hydrophobic contacts with the ligands are noted with red eyelashes.

residues are present at positions 117 and 146, respectively, in the human protein that are absent in ecTS (*1*). It is apparent that the N-terminus does not have a single conformation with a deep energy minimum. Different N-terminal extension lengths and/or different conformational states (active/inactive and/or open/close) do not induce an ordered structure of the N-terminus in either rat or human TSs. This is in contrast to the inserts, which are disordered in the native hTS in the inactive conformation and ordered in the ternary inhibitory

complexes whether in the closed (hTS) or open (rTS) conformations. Thus, the formation of a ternary complex leads to a well-ordered structure in the insert regions. This structure is quite compact and the enzyme in this conformation may be less likely to undergo degradation. This hypothesis is consistent with studies in which a decrease in the turnover of TS was observed in tumor cells exposed to TS inhibitors (*24*).

The formation of a covalent complex in the hTS/dUMP/raltitrexed structure, in contrast to a noncovalent complex reported for the analogous rTS complex, is not likely to be a result of differences in amino acid sequences. The hTS and rTS sequences are 93% identical if the disordered N-terminus is omitted. The analogous ecTS complex is covalent while the sequences of ecTS and hTS are only 55% identical. Perhaps, the low pH of the crystallization medium, 6.0, resulted in protonation of the catalytic cysteine and formation of a noncovalent complex in type 2 crystals of rTS/dUMP/raltitrexed, diffracting to 2.6 Å. However, for type 1 crystals, which were obtained at more alkaline pH but yielded only medium resolution 3.3 Å data, also a noncovalent complex was proposed. Regardless of the basis for the differences in the nature of the complexes, structures of mammalian TSs have been elucidated in three states along the catalytic pathway: unliganded and inactive, liganded, active and open; and liganded, active and closed. Our structure of a drug−receptor complex offers a superior model for further structure-based anti-cancer drug design.

REFERENCES

1. Carreras, C. W., and Santi, D. V. (1995) *Annu. Rev. Biochem. 64*, 721−762.
2. Hougton, P. J. (1999) in *Antifolate Drugs in Cancer Therapy* (Jackman, A. L., Ed.) pp 423−435, Humana Press, Totowa, NJ.
3. Reviewed in Rustum, Y. M., Harstrick, A., Cao, S., Vanhoefer, U., Yin, M. B., Wilke, H., and Seeber, S. (1997) *J. Clin. Oncol. 15*, 389−400.
4. Jackson, R. C. (1999) in *Antifolate Drugs in Cancer Therapy* (Jackman, A. L., Ed.) pp 1−12, Humana Press, Totowa, NJ.
5. Beale, P., and Clarke, S. (1999) in *Antifolate Drugs in Cancer Therapy* (Jackman, A. L., Ed.) pp 167−181, Humana Press, Totowa, NJ.
6. Hughes, L. R., Stephens, T. C., Boyle, F. T., and Jackman, A. L. (1999) in *Antifolate Drugs in Cancer Therapy* (Jackman, A. L., Ed.) pp 147−165, Humana Press, Totowa, NJ.
7. Rutenber, E. E., and Stroud, R. M. (1996) *Structure 4*, 1317−1324.
8. Sotelo-Mundo, R. R., Ciesla, J., Dzik, J. M., Rode, W., Maley, F., Maley, G. F., Hardy, L. W., and Monfort, W. R. (1999) *Biochemistry 38*, 1087−1094.
9. Schiffer, C. A., Clifton, I. J., Davisson, V. J., Santi, D. V., and Stroud, R. M. (1995) *Biochemistry 34*, 16279−16287.
10. Phan, J. Steadman, D. J., Koli, S., Ding, W. C., Minor, W., Dunlap, R. B., Berger, S. H., and Lebioda, L. (2001) (submitted for publication).
11. Dunlap, R. B., Harding, N. G. L., and Huennekens, F. M. (1971) *Biochemistry 10*, 88−97.
12. Steadman, D. J., Zhao, P.-S., Spencer, H. T., Dunlap, R. B., and Berger, S. H. (1998) *Biochemistry 37*, 7089−7095.
13. Wahba A. J., and Friedkin, M. (1961) *J. Biol. Chem. 236*, PC11−PC12.
14. Ellis, K. J., and Morrison, J. F. (1982) *Methods Enzymol. 87*, 405−426.
15. Zapf, J. W., Weir, M. S., Emerick, V., Villafranca, J. E., and Dunlap, R. B. (1993) *Biochemistry 32*, 9274−9281.
16. Otwinowski, Z., and Minor, W., (1997) *Methods Enzymol. 276*, 307−326.
17. Navaza, J. (1994) *Acta Crystallogr., Sect. A 50*, 157−163.
18. Collaborative Computational Project, Number 4 (1994) *Acta Crystallogr., Sect. D 50*, 760−763.
19. Brunger, A. T., Adams, P. D., Clore, G. M., Delano, W. L., Gros, P., Grosse-Kunstleve, R. W., Jiang, J.-S., Kuszewski, J., Nilges, M., Pannu, N. S., Read, R. J., Rice, L. M., Simonson, T., and Warren, G. L. (1998) *Acta Crystallogr., Sect. D 54*, 905−921.
20. Sack, J. S., and Quiocho, F. A., (1997) *Methods Enzymol. 277*, 158−173.
21. Kabsch, W. (1976) *Acta Crystallogr., Sect. A 32*, 922−923.
22. Kraulis, P. J. (1991) *J. Appl. Crystallogr. 24*, 946−950.
23. Hyatt, D. C., Maley, F., and Montfort, W. R. (1997) *Biochemistry 36*, 4585−4594.
24. Kitchens, M. E., Forsthoefel, A. M., Rafique, Z., Spencer, H. T., and Berger, F. G. (1999) *J. Biol. Chem. 274*, 12544−12547.
25. Kraulis, P. J. (1991) *J. Appl. Crystallogr. 24*, 946−950.
26. Wallace, A. C., Laskowski, R. A., and Thorton, J. M. (1995) *Protein Eng. 8*, 127−134.

BI002413I